



## Article (refereed) - postprint

---

Zhang, Xiuming; Wu, Yiyun; Liu, Xuejun; Reis, Stefan; Jin, Jiabin; Dragosits, Ulrike; Van Damme, Martin; Clarisse, Lieven; Whitburn, Simon; Coheur, Pierre-Francois; Gu, Baojing. 2017. **Ammonia emissions may be substantially underestimated in China.** *Environmental Science & Technology*, 51 (21). 12089-12096. <https://doi.org/10.1021/acs.est.7b02171>

© 2017 American Chemical Society

This version available <http://nora.nerc.ac.uk/518058/>

NERC has developed NORA to enable users to access research outputs wholly or partially funded by NERC. Copyright and other rights for material on this site are retained by the rights owners. Users should read the terms and conditions of use of this material at <http://nora.nerc.ac.uk/policies.html#access>

**This document is the final manuscript version of the journal article, incorporating any revisions agreed during the peer review process. There may be differences between this and the publisher's version. You are advised to consult the publisher's version if you wish to cite from this article.**

The definitive version is available at <http://pubs.acs.org/>

Contact CEH NORA team at  
[noraceh@ceh.ac.uk](mailto:noraceh@ceh.ac.uk)

**Ammonia emissions may be substantially underestimated in China**

Xiuming Zhang<sup>†,‡</sup>, Yiyun Wu<sup>‡</sup>, Xuejun Liu<sup>§</sup>, Stefan Reis<sup>#,‡</sup>, Jiabin Jin<sup>¶</sup>, Ulrike Dragosits<sup>#</sup>, Martin Van Damme<sup>Δ</sup>, Lieven Clarisse<sup>Δ</sup>, Simon Whitburn<sup>Δ</sup>, Pierre-François Coheur<sup>Δ</sup>, Baojing Gu<sup>†,Φ,⊥,\*</sup>

<sup>†</sup>Department of Land Management, Zhejiang University, Hangzhou 310058, People's Republic of China;

<sup>‡</sup>Policy Simulation Laboratory, Zhejiang University, Hangzhou 310058, People's Republic of China;

<sup>§</sup>College of Resources and Environmental Sciences, China Agricultural University, Beijing 100193, People's Republic of China;

<sup>#</sup>NERC Centre for Ecology & Hydrology, Bush Estate, Penicuik, Midlothian, EH260QB, United Kingdom;

<sup>‡</sup>University of Exeter Medical School, Knowledge Spa, Truro, TR1 3HD, United Kingdom;

<sup>¶</sup>International institute for earth system science, Nanjing University, Nanjing 210046, People's Republic of China;

<sup>Δ</sup>Université libre de Bruxelles (ULB), Atmospheric Spectroscopy, Service de Chimie Quantique et Photophysique CP 160/09, Avenue F.D. Roosevelt 50, 1050 Bruxelles, Belgium

<sup>Φ</sup>School of Agriculture and Food, The University of Melbourne, Victoria 3010, Australia

<sup>⊥</sup>Laboratory of Rural-Urban Construction Land Economical and Intensive Use, Ministry of Land and Resources, Beijing 100812, China

**\*Corresponding Author:**

Department of Land Management, Zhejiang University, Zijingang Campus, 866 Yuhangtang Road, Hangzhou 310058, PR China. Tel & Fax: +86 571 8898 2615. E-mail: [bjgu@zju.edu.cn](mailto:bjgu@zju.edu.cn)

34 **Abstract**

35 China is a global hotspot of atmospheric ammonia (NH<sub>3</sub>) emissions and, as a consequence,  
36 very high nitrogen (N) deposition levels are documented. However, previous estimates of  
37 total NH<sub>3</sub> emissions in China were much lower than inference from observed deposition  
38 values would suggest, highlighting the need for further investigation. Here, we  
39 reevaluated NH<sub>3</sub> emissions based on a mass balance approach, validated by N deposition  
40 monitoring and satellite observations, for China for the period of 2000 to 2015. Total NH<sub>3</sub>  
41 emissions in China increased from  $12.1 \pm 0.8$  Tg N yr<sup>-1</sup> in 2000 to  $15.6 \pm 0.9$  Tg N yr<sup>-1</sup> in  
42 2015 at an annual rate of 1.9%, which is approximately 40% higher than existing studies  
43 suggested. This difference is mainly due to more emission sources now having been  
44 included and NH<sub>3</sub> emission rates from mineral fertilizer application and livestock having  
45 been underestimated previously. Our estimated NH<sub>3</sub> emission levels are consistent with  
46 the measured deposition of NH<sub>x</sub> (including NH<sub>4</sub><sup>+</sup> and NH<sub>3</sub>) on land (11-14 Tg N yr<sup>-1</sup>) and  
47 the substantial increases in NH<sub>3</sub> concentrations observed by satellite measurements over  
48 China. These findings substantially improve our understanding on NH<sub>3</sub> emissions,  
49 implying that future air pollution control strategies have to consider the potentials of  
50 reducing NH<sub>3</sub> emission in China.

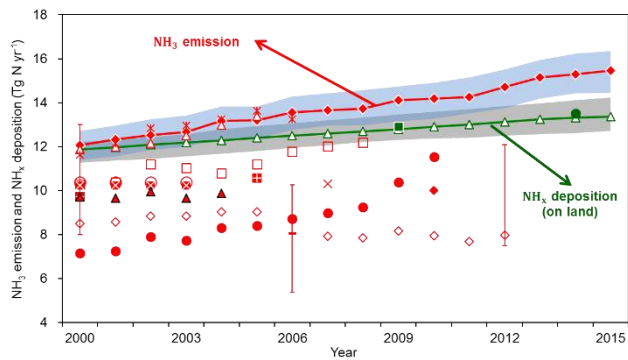
51

52 **Keywords:** fertilizer; nitrogen deposition; mass balance; satellite measurements;  
53 agriculture; temperature

54

55 TOC Art

56



57

58

## 59 INTRODUCTION

60 Nitrogen (N) plays an important role in all living systems and their environment.<sup>1, 2</sup>  
61 Reactive N ( $N_r$ ) released to the environment is dispersed by atmospheric and hydrologic  
62 transport processes and can accumulate in air, soils, vegetation, and groundwater.<sup>1</sup>  
63 Almost all emitted  $N_r$  in the forms of nitrogen oxides ( $NO_x$ , defined as the sum of all  
64 species that contained oxidized nitrogen) and ammonia ( $NH_3$ ) is transferred back to the  
65 Earth's surface within hours to days of its release.<sup>2</sup>  $NH_3$  emitted to the atmosphere is  
66 either deposited directly or transformed into an ammonium aerosol (e.g., ammonium  
67 nitrates and ammonium sulfate) often transported over long distances.<sup>3</sup> Two types of  $NH_x$   
68 ( $NH_3$  (gas) +  $NH_4^+$  (aerosol)) deposition usually occur: dry deposition of  $NH_3$  close to the  
69 emission sources,<sup>4, 5</sup> and wet deposition of  $NH_4^+$  that can occur at far distances downwind  
70 from the sources.<sup>6</sup> N biogeochemical cycles follow the principle of mass balance, and  
71 the  $N_r$  input to and output from the atmosphere system are normally balanced.<sup>7</sup> Therefore,  
72  $NH_x$  deposition fluxes are closely related to  $NH_3$  emissions. Galloway et al.<sup>8</sup> and Fowler  
73 et al.<sup>2</sup> elaborated the process of global N cycling and estimated that global  $NH_3$  emissions  
74 and  $NH_x$  deposition are in balance (Table 1). Global  $NH_x$  deposition depends strongly on  
75 total  $NH_3$  emissions, with the spatial distribution of emissions and atmospheric transport  
76 pathways affecting the downwind deposition fluxes to the oceans.<sup>9</sup>

77 Mainland China has long coastlines (total length about 18 000 km), bordering the  
78 Northwestern Pacific Ocean, which is primarily located downwind of emission sources  
79 on the Asian continent.<sup>10</sup> As a consequence, long-range transport will lead to a share of  
80 ammonium aerosols being deposited outside of China's land area, because prevailing  
81 wind directions and river catchment flows of China result in pollutants being carried from  
82 China to the North Pacific Ocean.<sup>11-13</sup> Figure S1 illustrates the sources and fates of  $NH_3$   
83 in China. It is noticeable that the Tibetan Plateau blocks most pollutant transfer into China  
84 from other countries in the west such as India though some evidence has emerged of  
85 transport of air pollutants across the Himalayas.<sup>14, 15</sup> China receives little  $NH_x$  from other  
86 countries through atmospheric circulation, but transports  $N_r$  to surrounding marine  
87 ecosystems, and is overall a net exporter of  $NH_x$  deposition.<sup>14</sup> Therefore, the flux of  $NH_x$   
88 deposition on land could be used to constrain the spatial and temporal variations of  $NH_3$   
89 emission in China.<sup>16</sup>

90 Over the past two decades, China has witnessed a substantial increase in  $N_r$  pollution  
91 and has been a global "hotspot" for both  $NH_3$  emissions and N deposition due to rapid  
92 increases in industrialization, urbanization and intensified agricultural production.<sup>7, 17, 18</sup>  
93 Rapid increases in atmospheric  $NH_3$  concentrations and the subsequent N depositions  
94 have various effects on ecosystems, such as soil acidification, water eutrophication,  
95 biodiversity loss and air pollution.<sup>19, 20</sup> Although many studies on emission inventories in  
96 general and  $NH_3$  emissions in particular have been conducted in China, large uncertainties  
97 and contradictory results were found in terms of spatial and temporal variations of  $NH_3$

emissions (e.g., Dong et al.<sup>21</sup>; Huang et al.<sup>22</sup>; Kang et al.<sup>23</sup>). Total estimates of NH<sub>3</sub> emissions available for China range from 7-8 Tg N yr<sup>-1</sup><sup>23,24</sup> to around 11-12 Tg N yr<sup>-1</sup>.<sup>25, 26</sup> Some studies<sup>24, 26</sup> recorded an increasing trend, while other studies<sup>23</sup> argued a downward trend of total NH<sub>3</sub> emission in China for the recent decade. Previous studies rarely used other data apart from ground-based concentration measurements for emission verification, such as N deposition monitoring or satellite observation to calibrate estimates and validate NH<sub>3</sub> inventories.

Recent studies have addressed the important role of NH<sub>3</sub> in the formation of fine particles (PM<sub>2.5</sub>) in China,<sup>27, 28</sup> putting more of an emphasis on the need to refine and better quantify NH<sub>3</sub> emissions and their contribution to air pollution, including for urban areas, in China. Thus, in this paper we aimed to (i) advance our understanding by designing a systematic framework for the analysis of NH<sub>3</sub> sources, emissions, and environmental fates in China; (ii) review and revise the NH<sub>3</sub> emission inventory from 2000 to 2015 in China with a mass balance approach; and (iii) evaluate the uncertainties attributed to NH<sub>3</sub> emissions by validation of NH<sub>x</sub> deposition and satellite measurements.

113

## 114 METHODS

**Datasets.** This study covers the entire land area of mainland China; Taiwan, Hong Kong, and Macao were excluded owing to data limitations. Data used in this study can be divided into two categories: (i) summary information for China such as population, GDP, land use, fertilizer use, crop/livestock production, and energy consumption in different sectors, all taken from the national data center<sup>29</sup> and FAO statistics<sup>30</sup>; (ii) parameters and coefficients used for the calculation of NH<sub>3</sub>-N fluxes, both obtained from synthesis of peer-reviewed literature and field measurements. We established multiple datasets for the calculation of NH<sub>x</sub> emissions from 2000 to 2015 in China on a provincial scale. Note that all the units of NH<sub>x</sub> fluxes have been converted to Tg N yr<sup>-1</sup>. Details about the selection criteria applied to and parameters and coefficients can be found in SI methods.

**Model Description.** We used the Coupled Human And Natural Systems (CHANS) model to quantify NH<sub>3</sub> fluxes within China. The CHANS model incorporates and integrates all N<sub>r</sub> fluxes and their interactions that can be identified, together with the linkages among subsystems (Figure S2). The basic principle of the CHANS model is mass balance for the whole system and each subsystem. A detailed description of CHANS can be found in Gu et al.<sup>31</sup> In this study, we focus on the atmosphere subsystem (AT) which receives NH<sub>3</sub> input from 13 subsystems and deposits NH<sub>x</sub> to land subsystems. In addition, it can also transfer NH<sub>x</sub> to or receive NH<sub>x</sub> from other countries/oceans through atmospheric circulation. The input of NH<sub>3</sub> is either larger or equal to the output of NH<sub>x</sub>. A summary of the main source categories comprised in the NH<sub>3</sub> emission inventory is listed in Table S1.

Meteorological conditions strongly influence the rate of NH<sub>3</sub> emissions.<sup>32, 33</sup> We

137 quantitatively estimate the impacts of climate change on NH<sub>3</sub> emission based on the  
 138 climate-dependent paradigm developed by Sutton et al.<sup>32</sup> This climate-dependent  
 139 paradigm is generally universal among regions, and can be used in China. In principle,  
 140 according to solubility and dissociation thermodynamics, NH<sub>3</sub> volatilization potential  
 141 nearly doubles for an increase of temperature by 5°C, equivalent to a Q<sub>10</sub> (the relative  
 142 increase over a range of 10°C) of 1–4.<sup>32</sup> Note that in this study, we only consider the  
 143 temperature-dependence effect on agricultural sources given that to date only few studies  
 144 have emerged in literature which thoroughly quantify the effect of temperature on non-  
 145 agricultural sectors.<sup>34</sup> Base on Sutton et al.,<sup>32</sup> an average Q<sub>10</sub> of 2 was used for NH<sub>3</sub> EFs  
 146 from fertilizer application across China; an average Q<sub>10</sub> of 1.25 was used for NH<sub>3</sub> EFs  
 147 from pigs, sows, poultry, rabbits, sheep and goats while an average Q<sub>10</sub> of 2.5 for cattle,  
 148 horses, donkeys, mules. Prior to the calibration of temperature-dependence effects, we  
 149 have summarized the average NH<sub>3</sub> EFs using correction coefficients for various factors.  
 150 Details on the approach can be found in SI text.

151 The annual average temperature for fifteen years (2000-2015) at 9.7°C across China  
 152 has been selected as a reference temperature and warmer or colder annual averages as a  
 153 proxy for calibration of the NH<sub>3</sub> emission. The calculation principles are as follow:

$$154 \quad AT_{IN} = \sum_{i=1}^{13} E_{Item,i} + AT_{IN}_{Import} \quad (1)$$

$$155 \quad E_{Item,i,j} = \sum_p EF_{i,j,p} \times f(T_{j,p}) \times AL_{i,j,p} \quad (2)$$

$$156 \quad f(T_{j,p}) = \frac{(Q_{10,j,p}-1)}{10} \times (T_j - T_0) + 1 \quad (3)$$

$$157 \quad AT_{OUT} = AT_{OUT}_{Dep} + AT_{OUT}_{Export} \quad (4)$$

$$158 \quad AT_{IN} \geq AT_{OUT} \quad (5)$$

159 where  $AT_{IN}$  and  $AT_{OUT}$  are the total NH<sub>x</sub> input to and output from atmosphere  
 160 subsystem;  $E_{Item,i,j}$  is the NH<sub>x</sub> emission from other 13 subsystems to atmosphere;  $i, j$   
 161 and  $p$  represent the subsystem, the year and the source type, respectively;  $EF_{i,j,p}$  is the  
 162 corresponding emission factor (EF);  $f(T_{j,p})$  represents a function of climate effect on  
 163 NH<sub>3</sub> emission;  $T_j$  is the annual average temperature (°C),  $T_0$  represents the fifteen  
 164 years (2000-2015) average temperature (9.7°C);  $Q_{10,j,p}$  stands for a temperature effect  
 165 on the NH<sub>3</sub> volatilization potential;  $AL_{i,j,p}$  is the activity data;  $AT_{OUT}_{Dep}$  is the NH<sub>x</sub>  
 166 deposition on land, including both dry and wet deposition.  $AT_{OUT}_{Export}$  is the NH<sub>x</sub>  
 167 transferred to surrounding areas (mainly to ocean) through atmospheric circulation that  
 168 advects NH<sub>x</sub> away from China.

169 **Uncertainty analysis.** Monte Carlo simulation was used to quantify the variability of the  
 170 NH<sub>3</sub> fluxes. In Monte Carlo simulations, random numbers are selected from the normal  
 171 or uniform distribution of input variables and a variation range is attributed to the  
 172 emission inventory. In order to thoroughly test the accuracy of the simulation results,  
 173 10,000 Monte Carlo simulations were executed to estimate the range of NH<sub>3</sub> emission

174 uncertainties for different sources. Meanwhile, the mass balance approach used in the  
175 CHANS model constrains the uncertainty ranges and helps to refine the overall  
176 uncertainty.<sup>7</sup> Details about the uncertainty assessment can be found in the SI text and  
177 tables.

178

## 179 RESULTS

180 **Total NH<sub>3</sub> emission in 2015.** The total NH<sub>3</sub> emission into the atmosphere was estimated  
181 at 15.6±0.9 Tg N in 2015 for China. Agricultural sources were the largest contributors  
182 (13.6±0.8 Tg N), accounting for 88% of total NH<sub>3</sub> emissions, with 5.8±0.3 Tg N and  
183 6.6±0.5 Tg N stemming from cropland and livestock, respectively. The majority of the  
184 NH<sub>3</sub> emissions from cropland originated from the application of mineral fertilizers  
185 (5.4±0.2 Tg N), and the rest from irrigation, agricultural soils, N-fixing crops, and  
186 composting of crop residues (Figure S3). An estimated 3.8±0.2 Tg N was emitted from  
187 livestock housing and manure storage. In addition, 2.8±0.3 Tg N was emitted from  
188 manure application to cropland, which in some studies has been attributed to cropland  
189 emissions.<sup>35, 36</sup>

190 The spatial distribution of NH<sub>3</sub> emissions on a provincial scale in 2015 is shown in  
191 Figure 1a, revealing a strong spatial variability and association with the distribution of  
192 arable land. High NH<sub>3</sub> emission densities above 50 kg N ha<sup>-1</sup> were concentrated across  
193 the North China Plain, where intensive agriculture for both crop production and animal  
194 husbandry are located. Sichuan Basin, Middle South China and Northeastern China also  
195 show high NH<sub>3</sub> emission densities. In contrast, low NH<sub>3</sub> emission densities of less than  
196 10 kg N ha<sup>-1</sup> were primarily found across western China, e.g. Tibet, Qinghai, Inner  
197 Mongolia and Gansu, which are characterized by dry regions with low agricultural  
198 production and little N fertilizer use.<sup>29</sup>

199 **Temporal trends of NH<sub>3</sub> emissions.** Total NH<sub>3</sub> emissions increased from 12.1±0.8 Tg N  
200 in 2000 to about 15.6 ± 0.9 Tg N in 2015 with an annual rate of 1.9% (statistically  
201 significant). ~85% of the inter-annual variations could be well explained by the changes  
202 of human activity levels (Figure S4), and the remaining 15% were attributed to air  
203 temperature changes during this period (Figure S5). Agriculture is the main emission  
204 source, accounting for ~87% of the total NH<sub>3</sub> emission in China, with on average, 43.1%  
205 (41.6-44.1%) contributed by livestock manure and 36.4% (35.0-38.3%) by fertilizer  
206 application. Non-agricultural sources account for only about 13% of total national NH<sub>3</sub>  
207 emissions, including humans responsible for 6.6% (5.1-8.8%), other sources (fuel  
208 combustion, waste disposal, traffic sources, chemical industry, urban green land)  
209 contributed to less than 2% (Figure S4).

210 **Uncertainty assessment.** The range of NH<sub>3</sub> emissions with a 95% confidence interval  
211 for 2000, 2005, 2010, 2015 was estimated at 11.4-12.7, 12.3-13.8, 13.3-14.9, and 14.5-  
212 16.6 Tg N yr<sup>-1</sup>, respectively (Figure 2). Uncertainty contribution and variation ranges of

213 different emission source sectors are presented in Table S14. Livestock manure and  
214 fertilizer application were identified as the key sources, with contributions to overall  
215 uncertainty of 43.1% and 36.4%, respectively.

216

## 217 **DISCUSSION**

218 **Validation by NH<sub>x</sub> deposition.** In contrast to the bottom-up estimates of NH<sub>3</sub> emission  
219 in current inventories, NH<sub>x</sub> deposition can be comparatively well constrained based on  
220 data from field monitoring. Based on our NH<sub>3</sub> emission estimations, we could derive the  
221 range of NH<sub>x</sub> deposition in mainland China ( $Dep_{derived} = NH_3 \text{ emission} - \text{exported} +$   
222  $\text{imported}$ , where exported NH<sub>3</sub> flux accounts for ~20% of NH<sub>3</sub> emission<sup>14</sup>, and imported  
223 N flux from outside contributed by foreign anthropogenic emissions is ~1 Tg N yr<sup>-110</sup>).  
224 The derived NH<sub>x</sub> deposition was calculated at 12.6 Tg N in 2010 (Figure 2).

225 To be directly comparable with the observation data of NH<sub>x</sub> deposition, Figure 2  
226 integrated the NH<sub>x</sub> deposition on land for China (data extracted from Liu et al.<sup>17</sup> and Xu  
227 et al.<sup>6</sup>). Liu et al.<sup>17</sup> and Xu et al.<sup>6</sup> conducted a comprehensive evaluation of N deposition  
228 dynamics across China (Figure S6) based on a Nationwide Nitrogen Deposition  
229 Monitoring Network (NNDMN). Result indicated a NH<sub>x</sub> deposition around 11-14 Tg N  
230 yr<sup>-1</sup> over land areas in China during 2000-2015, with a 12.9 Tg N in 2010. A range of  
231 additional studies based on N deposition monitoring data also support the estimated range  
232 of NH<sub>x</sub> deposition over China (Table 2). Therefore, the derived NH<sub>x</sub> deposition from our  
233 estimate of NH<sub>3</sub> emission agreed well with the observed NH<sub>x</sub> deposition over land areas  
234 in China.

235 It is noticeable from Figure 2 that the difference between NH<sub>3</sub> emissions and  
236 terrestrial NH<sub>x</sub> deposition increased in recent years. We assume that this can be attributed  
237 to the increased long-distance transport of NH<sub>x</sub> deposition to the ocean. Elevated NH<sub>x</sub>  
238 deposition rates found in the North and Northwestern Pacific Oceans<sup>11, 13</sup> demonstrates  
239 that the formation of ammonium sulphate and –nitrate extended the lifetime of NH<sub>3</sub> in the  
240 atmosphere, promoting its long-range transport to ocean.<sup>10</sup> This is in line with the  
241 observation that, despite the most recent reductions of NO<sub>x</sub> and SO<sub>2</sub> emissions<sup>37</sup> in China,  
242 the molar amount of (2SO<sub>2</sub>+NO<sub>x</sub>) still substantially exceeded that of NH<sub>3</sub> at least until  
243 2015 (Figure 3), suggesting that NH<sub>3</sub> emissions presented the limiting factor to the  
244 formation of ammonium aerosols. Thus, the increase of NH<sub>3</sub> emission would increase the  
245 formation of ammonium aerosols and the long-range transport to ocean during 2000-2015  
246 in China. It should be noted that while Figure 3 presents a mass balance limit to the  
247 relative components of each species, other factors, i.e. temperature, relative humidity, and  
248 aerosol composition could affect the limitations of aerosol formation,<sup>27</sup> and a full  
249 atmospheric chemistry transport model assessment would be needed to further assess  
250 limiting reagents.

251 **Validation by satellite observations.** Ground-based measurements of ambient NH<sub>3</sub> are

252 sparse and not always representative for a larger area. Satellites provide an alternative and  
253 are ideal to measure NH<sub>3</sub> spatial and temporal variability on global scale.<sup>38, 39</sup> Figure 1  
254 presents the spatial distributions of NH<sub>3</sub> emission and the NH<sub>3</sub> vertical column densities  
255 (VCDs) measured with the Infrared Atmospheric Sounding Interferometer (IASI) satellite  
256 for 2015 over China.<sup>40</sup> The spatial variability of our estimates of the NH<sub>3</sub> emission  
257 densities agree well with the IASI-NH<sub>3</sub> VCDs distribution, with the largest NH<sub>3</sub> emission  
258 density found in the North China Plain, Sichuan Basin and Northeastern China. Relatively  
259 high NH<sub>3</sub> VCDs could also be observed in Xinjiang by satellite IASI instrument, which  
260 is not captured by our emission map. There is little emission of SO<sub>2</sub> and NO<sub>x</sub> from  
261 industrial sources in Xinjiang compared to that in Eastern China.<sup>41</sup> Therefore, a reduced  
262 conversion rate to aerosol is expected. This, and the dry climate is probably responsible  
263 for a longer lifetime of NH<sub>3</sub> in the atmosphere in Xinjiang compared to other regions in  
264 China. This will lead, in those regions to a larger buildup of NH<sub>3</sub>, and hence larger  
265 observed columns and a larger qualitative discrepancy with the emission inventory.

266 Recently, Warner et al.<sup>33</sup> showed an increasing trend of NH<sub>3</sub> VCDs in China from  
267 2003 to 2015 with an increment of  $0.076 \pm 0.020$  ppbv (parts-per-billion by volume) per  
268 year ( $2.3\% \text{ yr}^{-1}$ ) using measurements of the Atmospheric InfraRed Souder (AIRS) satellite.  
269 This increasing trend of NH<sub>3</sub> VCDs in China agreed well with our results that showed an  
270 annual increase rate of 2.0% during the same period. Generally, the increased NH<sub>3</sub>  
271 emissions contributed to the variation in NH<sub>3</sub> VCDs. It suggested that the decreasing  
272 trends or trends with turning points of NH<sub>3</sub> emission from 2000 to 2015 found in previous  
273 studies are not accurate (Figure 2). For instance, a recent study by Kang et al.<sup>23</sup> estimated  
274 that total NH<sub>3</sub> emissions in China showed a downward trend from 8.5 Tg N in 2000 to  
275 8.0 Tg N in 2012, contradictory to the increasing trend found in satellite measurements.  
276 However, note that satellite concentrations should not be directly compared with  
277 emissions, as NH<sub>3</sub> columns are in addition to sources, determined by transport and sinks<sup>40,</sup>  
278 <sup>41</sup>. Hence, we suggest such data is primarily used for qualitative comparisons such as  
279 temporal trend analysis.

280 **Comparison with other studies.** Figure 2 indicates that our results estimated NH<sub>3</sub>  
281 emissions to be about 40% higher than previous studies suggested, majority of which  
282 estimated a lower amount of NH<sub>3</sub> emission than inference from observed NH<sub>x</sub> deposition  
283 would yield. Table 3 shows a quantitative comparison with previous studies from five  
284 main sources, and the differences are mainly arising from estimates of emissions from  
285 fertilizer use and livestock production. In addition, we included additional emission  
286 sources compared to other studies, such as grassland, aquaculture, traffic sources, urban  
287 vegetation, humans and pets, even though the latter contributed a relatively small  
288 proportion of total emissions (SI text).

289 The total amount of mineral fertilizer applied and emission factors (EFs) for NH<sub>3</sub>  
290 volatilization are two key factors that directly affect NH<sub>3</sub> emissions from N fertilizer

291 application. Compared to other studies, the difference regarding estimated activity data  
292 (i.e. amount of fertilizer uses) is less than 5%. However, the final corrected EFs (16.2-  
293 18.4%, average 17.0%) used in this study were about 16.6% higher than those used in  
294 other studies (Figure S10, average 14.6%). The majority of previous inventories compiled  
295 for China used constant European-based emission factors (EFs) (e.g., Dong et al.<sup>21</sup>; Kang  
296 et al.<sup>23</sup>), and did not adjust for specific agricultural practices, environmental conditions  
297 and climatological factors. Some studies<sup>23, 42</sup> adopted much lower EFs (Figure S10,  
298 average 12.8%) because they believed that an anticipated shift of dominant fertilizer types  
299 from ABC to urea would substantially reduce the NH<sub>3</sub> emission.<sup>23, 42</sup> In fact, the actual  
300 EFs are substantially influenced by the method of fertilizer application used. ABC is  
301 normally applied as base fertilizer with deep placement that results in a lower EF, while  
302 urea is widely used for top-dressing and surface application<sup>43, 44</sup>. The percentage of  
303 topdressing for urea is higher than that for ABC (Table S5) and as such is likely to  
304 substantially increase NH<sub>3</sub> emissions in China.<sup>44</sup> Therefore, the gradual shift of fertilizer  
305 type from ABC to urea would not significantly change the overall NH<sub>3</sub> EF for fertilizer  
306 application in China.

307 A recent meta-analysis<sup>45</sup> on the topic of NH<sub>3</sub> volatilization from global fertilizer use  
308 indicates that the global average percentage of N lost as NH<sub>3</sub> was 17.6%. The NH<sub>3</sub>  
309 volatilization rate for China is expected to be higher than this value, given its higher  
310 application rate and lower N use efficiency considering the fact that most farming is done  
311 on smallholder farms, which rely mainly on family labor and are traditionally slow to  
312 adapt technical improvements such as 4R fertilization management.<sup>46</sup>

313 Table 3 indicates that the total NH<sub>3</sub> emissions from livestock calculated in this study  
314 were 1.4 Tg N yr<sup>-1</sup> higher than other studies on average, such as REAS2.1,<sup>26</sup> Xu et al.<sup>35</sup>  
315 and EDGARv4.3.1.<sup>24</sup> The EFs for livestock used in this study are compared with other  
316 studies in Figure S6. In fact, due to the absence of closed systems to produce liquid  
317 manure, the air-dry process used to produce manure for field application in China results  
318 in high emissions of NH<sub>3</sub> from livestock production.<sup>47</sup> In addition, the backyard and  
319 small-scale livestock farms still dominate animal production in China, which is difficult  
320 to supervise the NH<sub>3</sub> emission from livestock production and further introduce advanced  
321 technologies to reduce the NH<sub>3</sub> emission due to high costs.<sup>47</sup> Therefore, even assuming  
322 the same excretion rate for livestock, the resulting NH<sub>3</sub> emission rate is expected to be  
323 higher in China because manure management systems are not as advanced as developed  
324 countries.

325 **Uncertainty and Limitation.** To estimate the uncertainty range on a national scale is  
326 challenging given the large spatial variability of EFs of NH<sub>3</sub>. A simple additive approach  
327 for all uncertainties from each region and source would undoubtedly exaggerate the  
328 overall uncertainty. The NH<sub>3</sub> emissions in this study were calculated based on a full life-  
329 cycle analysis, which is a framework to quantify and track the trajectory of all nitrogen

330 fluxes in the CHANS.<sup>7,31</sup> Thus, the uncertainty range inherent to the CHANS model could  
331 be well constrained by the mass balance calculation in all the 13 subsystems, combining  
332 with Monte Carlo simulations.

333 However, we have identified several limitations of this study, especially for the major  
334 emission sources of N fertilizer and livestock. The actual EFs for fertilizer application are  
335 substantially influenced by many parameters, including meteorological conditions, soil  
336 properties, fertilizer application methods, application rate, fertilizer type and so on.<sup>48</sup>  
337 However, generating a matching dataset of human activities data (e.g., N fertilizer  
338 application rate) with the same degree of detail and resolution on national scale is outside  
339 the scope of this study. At the same time, the influence of these factors on NH<sub>3</sub> emission  
340 at a large scale has not yet been well studied and quantified, to our knowledge. Therefore,  
341 it is difficult to integrate all the factors into the CHANS and comprehensively quantify  
342 the effects of those factors. Future work to build comprehensive datasets including both  
343 spatial and temporal variations of the key influencing factors would help to refine the  
344 results.

345 In addition, we assume there is no significant inter-annual change in the percentage  
346 of intensive rearing systems, manure management practice which is typically affected by  
347 many factors, including the housing structure, manure storage system, spreading  
348 technique, and so on<sup>49</sup>. However, manure management practices in China have been  
349 subject to great changes over the time period of 2000-2015,<sup>29</sup> hence additional  
350 uncertainties may be introduced due to using constant parameters for livestock manure  
351 during the study period<sup>23</sup>.

352 Some uncertainties may still exist in the observed NH<sub>x</sub> deposition used in this study  
353 due to the relatively limited number of sampling sites. In addition, NH<sub>3</sub> deposition may  
354 be overestimated at rural sites with relatively high canopy compensation points as a result  
355 of fertilized croplands or vegetation<sup>6</sup>. Furthermore, there may also be large uncertainties  
356 arising from comparison with satellite data, because observed differences between  
357 ammonia emission and NH<sub>3</sub> VCDs remain unclear to some extent, for instance, in  
358 locations such as Xinjiang. These uncertainties may affect the validation of NH<sub>3</sub>  
359 emissions in this paper.

360 **Outlook.** Refining the NH<sub>3</sub> emission inventory datasets with high spatiotemporal  
361 resolution is crucial for the assessment of future policy implications with regard to  
362 mitigation options. This paper highlights that the overall amount of NH<sub>3</sub> emissions may  
363 be substantially underestimated in China (Figure 2). However, we still lack a substantial  
364 amount of information on spatial resolution at regional to local scales, as well as future  
365 changes, which are decision making. Further work is still required to increase the  
366 reliability and accuracy of NH<sub>3</sub> emission inventory datasets, underpinned by high-  
367 resolution observations, process-based experiments and model-data assimilation to fully  
368 quantify more realistic NH<sub>3</sub> emissions. This can enhance our understanding on the  
369 variation of NH<sub>3</sub> emission and its driving forces.

370 Furthermore, NH<sub>3</sub> plays a crucial role in the formation of secondary inorganic  
371 aerosols (SIAs) that are the predominant components of fine particles in China.<sup>20</sup>

372 However, until now no control strategies have yet been implemented for NH<sub>3</sub> emissions  
373 in China. Effective strategies for the reduction of NH<sub>3</sub> emissions in China are thus  
374 urgently needed given a 40% higher NH<sub>3</sub> emission than previous thoughts. In support of  
375 such strategies, a comprehensive and accurate NH<sub>3</sub> emission inventory is also vital to  
376 future air pollution prevention and control in China, which can be integrated into air  
377 quality model and serve as a baseline toward tracking emission trends, developing  
378 mitigation strategies, and assessing progress.

379

### 380 Acknowledgments

381 This work was supported in part by the National Key Research and Development Project  
382 of China (2016YFC0207906); National Natural Science Foundation of China (No.  
383 41773068 and 41425007); the Fundamental Research Funds for the Central Universities  
384 (No. 581280\*172220261/010); the Open Fund of Key Laboratory of Nonpoint Source  
385 Pollution Control, Ministry of Agriculture, China (1610132016005); the Discovery Early  
386 Career Researcher Award by the Australian Research Council (DE170100423); and the  
387 Newton Fund via UK BBSRC/NERC (BB/N013484/1) for the UK-China Virtual Joint  
388 Centre on Nitrogen “N-Circle”.

389

### 390 Note

391 The authors declare no competing financial interest.

392

### 393 Supporting Information Available

394 The Supporting Information includes is available free of charge on the ACS  
395 Publications website.

396 Text S1–4, Table S1–16 and Figure S1–9 (PDF).

397

## 398 REFERENCES

399 (1) Galloway, J. N.; Townsend, A. R.; Erisman, J. W.; Bekunda, M.; Cai, Z.; Freney, J. R.; Martinelli, L.  
400 A.; Seitzinger, S. P.; Sutton, M. A. Transformation of the Nitrogen Cycle: Recent Trends, Questions, and  
401 Potential Solutions. *Science* **2008**, *320* (5878), 889-892.

402 (2) Fowler, D.; Coyle, M.; Skiba, U.; Sutton, M. A.; Cape, J. N.; Reis, S.; Sheppard, L. J.; Jenkins, A.;  
403 Grizzetti, B.; Galloway, J. N.; et al. The global nitrogen cycle in the twenty-first century. *Philos. Trans. R.*  
404 *Soc., B* **2013**, *368* (1621), 20130164.

405 (3) Kirkby, J.; Curtius, J.; Almeida, J.; Dunne, E.; Duplissy, J.; Ehrhart, S.; Franchin, A.; Gagné, S.; Ickes,  
406 L.; Kürten, A.; et al. Role of sulphuric acid, ammonia and galactic cosmic rays in atmospheric aerosol  
407 nucleation. *Nature* **2011**, *476* (7361), 429-433.

408 (4) Vogt, E.; Dragosits, U.; Braban, C. F.; Theobald, M. R.; Dore, A. J.; van Dijk, N.; Tang, Y. S.;  
409 McDonald, C.; Murray, S.; Rees, R. M.; et al. Heterogeneity of atmospheric ammonia at the landscape scale  
410 and consequences for environmental impact assessment. *Environ. Pollut.* **2013**, *179* (8), 120-131.

411 (5) Dragosits, U.; Theobald, M. R.; Place, C. J.; Lord, E.; Webb, J.; Hill, J.; ApSimon, H. M.; Sutton, M.

- 412 A. Ammonia emission, deposition and impact assessment at the field scale: a case study of sub-grid spatial  
413 variability. *Environ. Pollut.* **2002**, *117* (1), 147-158.
- 414 (6) Xu, W.; Luo, X. S.; Pan, Y. P.; Zhang, L.; Tang, A. H.; Shen, J. L.; Zhang, Y.; Li, K. H.; Wu, Q. H.;  
415 Yang, D. W.; et al. Quantifying atmospheric nitrogen deposition through a nationwide monitoring network  
416 across China. *Atmos. Chem. Phys.* **2015**, *15* (21), 12345-12360.
- 417 (7) Gu, B.; Ju, X.; Chang, J.; Ge, Y.; Vitousek, P. M. Integrated reactive nitrogen budgets and future trends  
418 in China. *Proc. Natl. Acad. Sci. U. S. A.* **2015**, *112* (28), 8792-8797.
- 419 (8) Galloway, J. N.; Dentener, F. J.; Capone, D. G.; Boyer, E. W.; Howarth, R. W.; Seitzinger, S. P.; Asner,  
420 G. P.; Cleveland, C. C.; Green, P. A.; Holland, E. A.; et al. Nitrogen cycles: past, present, and future.  
421 *Biogeochemistry* **2004**, *70* (2), 153-226.
- 422 (9) Doney, S. C.; Mahowald, N.; Lima, I.; Feely, R. A.; Mackenzie, F. T. Impact of anthropogenic  
423 atmospheric nitrogen and sulfur deposition on ocean acidification and the inorganic carbon system. *Proc.*  
424 *Natl. Acad. Sci. U. S. A.* **2007**, *104* (34), 14580-14585.
- 425 (10) Luo, X. S.; Tang, A. H.; Shi, K.; Wu, L. H.; Li, W. Q.; Shi, W. Q.; Shi, X. K.; Erisman, J. W.; Zhang,  
426 F. S.; Liu, X. J. Chinese coastal seas are facing heavy atmospheric nitrogen deposition. *Environ. Res. Lett.*  
427 **2014**, *2014* (9), 1-10.
- 428 (11) Kim, I.; Lee, K.; Gruber, N.; Karl, D. M.; Bullister, J. L.; Yang, S.; Kim, T. Increasing anthropogenic  
429 nitrogen in the North Pacific Ocean. *Science* **2014**, *346* (6213), 1100-1102.
- 430 (12) Zhao, Y.; Zhang, L.; Pan, Y.; Wang, Y.; Paulot, F.; Henze, D. K. Atmospheric nitrogen deposition to  
431 the northwestern Pacific: seasonal variation and source attribution. *Atmos. Chem. Phys.* **2015**, *15* (18),  
432 10905-10924.
- 433 (13) Kim, T.; Lee, K.; Najjar, R. G.; Jeong, H.; Jeong, H. J. Increasing N abundance in the Northwestern  
434 Pacific Ocean due to atmospheric nitrogen deposition. *Science* **2011**, *334* (6055), 505-509.
- 435 (14) Zhao, Y.; Zhang, L.; Chen, Y.; Liu, X.; Xu, W.; Pan, Y.; Duan, L. Atmospheric nitrogen deposition to  
436 China: A model analysis on nitrogen budget and critical load exceedance. *Atmos. Environ.* **2017**, *153*, 32-  
437 40.
- 438 (15) Zheng, J.; Hu, M.; Du, Z.; Shang, D.; Gong, Z.; Qin, Y.; Fang, J.; Gu, F.; Li, M.; Peng, J.; et al.  
439 Influence of biomass burning from South Asia at a high-altitude mountain receptor site in China. *Atmos.*  
440 *Chem. Phys.* **2017**, *17* (11), 6853-6864.
- 441 (16) Paulot, F.; Jacob, D. J.; Pinder, R. W.; Bash, J. O.; Travis, K.; Henze, D. K. Ammonia emissions in  
442 the United States, European Union, and China derived by high-resolution inversion of ammonium wet  
443 deposition data: Interpretation with a new agricultural emissions inventory (MASAGE\_NH<sub>3</sub>). *J. Geophys.*  
444 *Res. Atmos.* **2014**, *119* (7), 4343-4364.
- 445 (17) Liu, X.; Zhang, Y.; Han, W.; Tang, A.; Shen, J.; Cui, Z.; Vitousek, P.; Erisman, J. W.; Goulding, K.;  
446 Christie, P.; et al. Enhanced nitrogen deposition over China. *Nature* **2013**, *494* (7438), 459-462.
- 447 (18) Liu, L.; Zhang, X.; Wang, S.; Lu, X.; Ouyang, X. A review of spatial variation of inorganic nitrogen  
448 (N) wet deposition in China. *PLoS ONE* **2016**, *11* (1), e0146051.
- 449 (19) Hernández, D. L.; Vallano, D. M.; Zavaleta, E. S.; Tzankova, Z.; Pasari, J. R.; Weiss, S.; Selmants, P.  
450 C.; Morozumi, C. Nitrogen pollution is linked to US listed species declines. *BioScience* **2016**, *66* (3), 213-  
451 222.
- 452 (20) Fu, X.; Wang, S.; Xing, J.; Zhang, X.; Wang, T.; Hao, J. Increasing ammonia concentrations reduce  
453 the effectiveness of particle pollution control achieved via SO<sub>2</sub> and NO<sub>x</sub> emissions reduction in East China.  
454 *Environ. Sci. Technol. Lett.* **2017**, *4* (6), 221-227.

- 455 (21) Dong, W. X.; Xing, J.; Wang, S. X. Temporal and spatial distribution of anthropogenic ammonia  
456 emissions in China:1994-2006. *Environ. Sci.* **2010**, *31* (7), 1457-1463 (in Chinese).
- 457 (22) Huang, X.; Song, Y.; Li, M.; Li, J.; Huo, Q.; Cai, X.; Zhu, T.; Hu, M.; Zhang, H. A high-resolution  
458 ammonia emission inventory in China. *Global Biogeochem. Cycles* **2012**, *26* (1), 239256.
- 459 (23) Kang, Y.; Liu, M.; Song, Y.; Huang, X.; Yao, H.; Cai, X.; Zhang, H.; Kang, L.; Liu, X.; Yan, X.; et  
460 al. High-resolution ammonia emissions inventories in China from 1980 to 2012. *Atmos. Chem. Phys.* **2016**,  
461 *16* (4), 2043-2058.
- 462 (24) Emissions Database for Global Atmospheric Research (EDGAR v4.3.1).  
463 <http://edgar.jrc.ec.europa.eu/overview.php?v=431> (accessed July 6, 2016).
- 464 (25) Wang, S. W.; Liao, J. H.; Yu-Ting, H. U.; Yan, X. Y. A preliminary inventory of NH<sub>3</sub>-N emission and  
465 its temporal and spatial distribution of China. *J. Agro-Environ. Sci.* **2009**, *28* (3), 619-626 (in Chinese).
- 466 (26) Kurokawa, J.; Ohara, T.; Morikawa, T.; Hanayama, S.; Janssens-Maenhout, G.; Fukui, T.; Kawashima,  
467 K.; Akimoto, H. Emissions of air pollutants and greenhouse gases over Asian regions during 2000–2008:  
468 Regional Emission inventory in Asia (REAS) version 2. *Atmos. Chem. Phys.* **2013**, *13* (21), 11019-11058.
- 469 (27) Wang, G.; Zhang, R.; Gomez, M. E.; Yang, L.; Levy Zamora, M.; Hu, M.; Lin, Y.; Peng, J.; Guo, S.;  
470 Meng, J.; et al. Persistent sulfate formation from London Fog to Chinese haze. *Proc. Natl. Acad. Sci. U. S.*  
471 *A.* **2016**, *113* (48), 13630-13635.
- 472 (28) Wu, Y.; Gu, B.; Erisman, J. W.; Reis, S.; Fang, Y.; Lu, X.; Zhang, X. PM<sub>2.5</sub> pollution is substantially  
473 affected by ammonia emissions in China. *Environ. Pollut.* **2016**, *218*, 86-94.
- 474 (29) The National Bureau of statistics of the People's Republic of China; *China Statistical Yearbook (2001-*  
475 *2016)*; China Statistics Press: Beijing, China, 2016.
- 476 (30) FAOStat: Food and Agriculture Data, Food and Agriculture Organization.  
477 <http://faostat3.fao.org/home/E> (accessed December 10, 2015).
- 478 (31) Gu, B.; Ge, Y.; Ren, Y.; Xu, B.; Luo, W.; Jiang, H.; Gu, B.; Chang, J. Atmospheric Reactive Nitrogen  
479 in China: Sources, Recent Trends, and Damage Costs. *Environ. Sci. Technol.* **2012**, *46* (17), 9420-9427.
- 480 (32) Sutton, M. A.; Reis, S.; Riddick, S. N.; Dragosits, U.; Nemitz, E.; Theobald, M. R.; Tang, Y. S.; Braban,  
481 C. F.; Vieno, M.; Dore, A. J.; et al. Towards a climate-dependent paradigm of ammonia emission and  
482 deposition. *Philos. Trans. R. Soc., B* **2013**, *368* (1621), 20130166.
- 483 (33) Warner, J. X.; Dickerson, R. R.; Wei, Z.; Strow, L. L.; Wang, Y.; Liang, Q. Increased atmospheric  
484 ammonia over the world's major agricultural areas detected from space. *Geophys. Res. Lett.* **2017**, *44* (6),  
485 2875-2884.
- 486 (34) Meng, W.; Zhong, Q.; Yun, X.; Zhu, X.; Huang, T.; Shen, H.; Chen, Y.; Chen, H.; Zhou, F.; Liu, J.;  
487 et al. Improvement of a global high-resolution ammonia emission inventory for combustion and industrial  
488 sources with new data from the residential and transportation sectors. *Environ. Sci. Technol.* **2017**, *51* (5),  
489 2821-2829.
- 490 (35) Xu, P.; Liao, Y. J.; Lin, Y. H.; Zhao, C. X.; Yan, C. H.; Cao, M. N.; Wang, G. S.; Luan, S. J. High-  
491 resolution inventory of ammonia emissions from agricultural fertilizer in China from 1978 to 2008. *Atmos.*  
492 *Chem. Phys.* **2016**, *16* (3), 1207-1218.
- 493 (36) Xu, P.; Zhang, Y. S.; Gong, W. W.; Hou, X. K.; Kroeze, C.; Gao, W.; Luan, S. J. An inventory of the  
494 emission of ammonia from agricultural fertilizer application in China for 2010 and its high-resolution  
495 spatial distribution. *Atmos. Environ.* **2015**, *115*, 141-148.
- 496 (37) Liu, F.; Zhang, Q.; van DerA, R. J.; Zheng, B.; Tong, D.; Yan, L.; Zheng, Y.; He, K. Recent reduction  
497 in NO<sub>x</sub> emissions over China: synthesis of satellite observations and emission inventories. *Environ. Res.*

- 498 *Lett.* **2016**, *2016* (11), 114002.
- 499 (38) Clarisse, L.; Clerbaux, C.; Dentener, F.; Hurtmans, D.; Coheur, P. Global ammonia distribution derived  
500 from infrared satellite observations. *Nature Geosci.* **2009**, *2* (7), 479-483.
- 501 (39) Van Damme, M.; Erisman, J. W.; Clarisse, L.; Dammers, E.; Whitburn, S.; Clerbaux, C.; Dolman, A.  
502 J.; Coheur, P. F. Worldwide spatiotemporal atmospheric ammonia (NH<sub>3</sub>) columns variability revealed by  
503 satellite. *Geophys. Res. Lett.* **2015**, *42* (20), 8660-8668.
- 504 (40) Whitburn, S.; Van Damme, M.; Clarisse, L.; Bauduin, S.; Heald, C. L.; Hadji-Lazaro, J.; Hurtmans,  
505 D.; Zondlo, M. A.; Clerbaux, C.; Coheur, P. F. A flexible and robust neural network IASI-NH<sub>3</sub> retrieval  
506 algorithm. *J. Geophys. Res. Atmos.* **2016**, *121* (11), 6581-6599.
- 507 (41) Liu, L.; Zhang, X.; Xu, W.; Liu, X.; Lu, X.; Wang, S.; Zhang, W.; Zhao, L. Ground Ammonia  
508 Concentrations over China Derived from Satellite and Atmospheric Transport Modeling. *Remote Sens.*  
509 **2017**, *9* (5), 467.
- 510 (42) Zhang, Y.; Luan, S.; Chen, L.; Shao, M. Estimating the volatilization of ammonia from synthetic  
511 nitrogenous fertilizers used in China. *J. Environ. Manage.* **2011**, *92* (3), 480-493.
- 512 (43) Wang, J. Q.; Wen-Qi, M. A.; Jiang, R. F.; Zhang, F. S. Analysis about amount and ratio of basal  
513 fertilizer and topdressing fertilizer on rice, wheat, maize in China. *Chin. J. Soil Sci.* **2008**, *39* (2), 329-333  
514 (in Chinese).
- 515 (44) Fu, X.; Wang, S. X.; Ran, L. M.; Pleim, J. E.; Cooter, E.; Bash, J. O.; Benson, V.; Hao, J. M. Estimating  
516 NH<sub>3</sub> emissions from agricultural fertilizer application in China using the bi-directional CMAQ model  
517 coupled to an agro-ecosystem model. *Atmos. Chem. Phys.* **2015**, *15* (12), 6637-6649.
- 518 (45) Pan, B.; Lam, S. K.; Mosier, A.; Luo, Y.; Chen, D. Ammonia volatilization from synthetic fertilizers  
519 and its mitigation strategies: A global synthesis. *Agric., Eco. & Environ.* **2016**, *232*, 283-289.
- 520 (46) Ju, X.; Gu, B.; Wu, Y.; Galloway, J. N. Reducing China's fertilizer use by increasing farm size. *Global*  
521 *Environ. Chang.* **2016**, *41*, 26-32.
- 522 (47) Bai, Z. H.; Ma, L.; Qin, W.; Chen, Q.; Oenema, O.; Zhang, F. S. Changes in Pig Production in China  
523 and Their Effects on Nitrogen and Phosphorus Use and Losses. *Environ. Sci. Technol.* **2014**, *48* (21), 12742-  
524 12749.
- 525 (48) Fu, X.; Wang, S. X.; Ran, L. M.; Pleim, J. E.; Cooter, E.; Bash, J. O.; Benson, V.; Hao, J. M. Estimating  
526 NH<sub>3</sub> emissions from agricultural fertilizer application in China using the bi-directional CMAQ model  
527 coupled to an agro-ecosystem model. *Atmos. Chem. Phys.* **2015**, *15* (12), 6637-6649.
- 528 (49) Bai, Z.; Ma, L.; Jin, S.; Ma, W.; Velthof, G. L.; Oenema, O.; Liu, L.; Chadwick, D.; Zhang, F. Nitrogen,  
529 Phosphorus, and Potassium Flows through the Manure Management Chain in China. *Environ. Sci. Technol.*  
530 **2016**, *50* (24), 13409-13418.
- 531 (50) Jia, Y.; Yu, G.; Gao, Y.; He, N.; Wang, Q.; Jiao, C.; Zuo, Y. Global inorganic nitrogen dry deposition  
532 inferred from ground- and space-based measurements. *Sci. Rep.* **2016**, *6* (19810), 1-11.
- 533 (51) Jia, Y.; Yu, G.; He, N.; Zhan, X.; Fang, H.; Sheng, W.; Zuo, Y.; Zhang, D.; Wang, Q. Spatial and  
534 decadal variations in inorganic nitrogen wet deposition in China induced by human activity. *Sci. Rep.* **2014**,  
535 *4* (3763), 1-7.
- 536 (52) Zhu, J.; He, N.; Wang, Q.; Yuan, G.; Wen, D.; Yu, G.; Jia, Y. The composition, spatial patterns, and  
537 influencing factors of atmospheric wet nitrogen deposition in Chinese terrestrial ecosystems. *Sci. Total.*  
538 *Environ.* **2015**, *2015* (511), 777-785.
- 539 (53) Van Damme, M.; Whitburn, S.; Clarisse, L.; Clerbaux, C.; Hurtmans, D.; Coheur, P. F. Version 2 of  
540 the IASI NH<sub>3</sub> neural network retrieval algorithm; near-real time and reanalysed datasets. *Atmos. Meas.*

541 *Tech. Disc.* **2017**, doi:10.5194/amt-2017-239.

542 (54) China statistical yearbook on environment (2001-2015). <http://datacenter.mep.gov.cn>.

543 .

544

545

546 **Table 1 N input, NH<sub>3</sub> emission and deposition in the world and China**

	World			China
	1860 <sup>a</sup>	early-1990s <sup>a</sup>	2010 <sup>b</sup>	2010 <sup>c</sup>
<b>Total terrestrial N input</b>	<b>135</b>	<b>263</b>	<b>278</b>	<b>61.3</b>
Fertilizer production	0	100	120	37.1
NBNF	120	107	58	7.1
CBNF	15	31.5	60	4.6
NO <sub>x</sub> -FF	0.3	24.5	40	6.6
<b>NH<sub>3</sub> emission</b>	<b>20.5</b>	<b>58.2</b>	<b>69</b>	<b>14.0</b>
Terrestrial	14.9	52.6	60	14.0
Marine	5.6	5.6	9	-
<b>NH<sub>x</sub> deposition</b>	<b>18.8</b>	<b>56.7</b>	<b>64</b>	<b>13.8</b>
Terrestrial	10.8	38.7	40	13.1 <sup>d</sup>
Marine	8	18	24	0.7 <sup>e</sup>

547 Unit: Tg N yr<sup>-1</sup>; Fertilizer production, Haber–Bosch N fixation for fertilizer use; NBNF,  
 548 natural biological N fixation; CBNF, cultivated biological N fixation; NO<sub>x</sub>-FF, NO<sub>x</sub>  
 549 emission via fossil fuel combustion.

550 a, adapted from Galloway et al.<sup>8</sup>

551 b, adapted from Fowler et al.<sup>2</sup>

552 c, adapted from Gu et al.<sup>7</sup>

553 d, adapted from Liu et al.<sup>17</sup>

554 e, adapted from Luo et al.<sup>10</sup>

555

556 **Table 2 NH<sub>x</sub> deposition on land area of China.**

Studies	Base year	Deposition density (kg N ha <sup>-1</sup> yr <sup>-1</sup> )			Total deposition (Tg N yr <sup>-1</sup> )
		Dry	Wet	Total	
Jia et al. <sup>50, 51</sup>	2000-2009	-	-	13.9	12.9
Liu et al. <sup>17</sup>	2000-2010	-	-	14.3	13.3
Xu et al. <sup>6</sup>	2010-2014	-	-	14.5	13.5
Liu et al. <sup>18</sup>	2003-2014	-	6.8	-	6.3*
Jia et al. <sup>51</sup>	2005-2014	6.1	-	-	5.7*
Zhu et al. <sup>52</sup>	2013	-	7.3	-	6.8*

557 \* Only wet or dry NH<sub>x</sub> deposition.

558

559 **Table 3 Comparison of NH<sub>3</sub> emissions with other studies**

Studies	Year	Total	Fertilizer	Livestock	Humans	Burning	Others
REAS	2000	10.3 // +1.8	4.2 // -0.2	4.2 // +0.9	1.2 // -0.1	0.5 // -0.3	0.2 // +1.4
Wang et al.	2005	13.4 // -0.2	4.2 // +0.1	5.8 // -0.1	0.2 // +0.8	-	3.3 // -1.2
Huang et al.	2006	8.1 // +5.1	2.6 // +2.1	4.4 // +1.3	0.2 // +0.7	0.1 // +0.2	0.8 // +0.8
Dong et al.	2006	13.2 // +0.1	7.2 // -2.5	5.4 // +0.3	0.5 // +0.4	-	0.1 // +1.8
Paulot et al.	2007	8.4 // +5.1	3.0 // +1.9	4.8 // +0.9	-	-	0.6 // +2.3
Xu et al.	2008	-	2.7 // +2.0	3.1 // +2.8	0.6 // +0.3	-	-
EDGAR	2010	11.5 // +2.3	4.9 // -0.1	4.2 // +1.9	-	-	0.7 // +2.4
Xu et al.	2010	-	3.7 // +1.2	4.2 // +2.0	0.4 // +0.4	-	-
Fu et al.	2011	-	2.5 // +2.3	-	-	-	-
Kang et al.	2012	8.0 // +6.7	2.3 // +2.7	4.1 // +2.4	0.1 // +0.7	0.3 // -0.1	1.1 // +1.1

560 Note that before the “//” is the previous studies, after the “//” is the difference of our  
561 result with previous studies, +xx or -yy in red/green colors in each column represents  
562 higher or lower value in our study than previous research; “-” means unavailable data;  
563 all the units of NH<sub>3</sub> emission have been converted to the Tg N yr<sup>-1</sup>.

564 REAS<sup>26</sup>

565 Wang et al.<sup>25</sup>

566 Huang et al.<sup>22</sup>

567 Dong et al.<sup>21</sup>

568 Paulot et al.<sup>16</sup>

569 Xu et al.<sup>35</sup>

570 EDGAR<sup>24</sup>

571 Xu et al.<sup>36</sup>

572 Fu et al.<sup>44</sup>

573 Kang et al.<sup>23</sup>

574

575 **Figure Legend**

576 **Figure 1 Validation by satellite observations (IASI) on spatial patterns.** (a) The  
577 spatial patterns of NH<sub>3</sub> emission density in mainland China in 2015; (b) Mean IASI-  
578 NH<sub>3</sub> VCDs (10<sup>16</sup> molec cm<sup>-2</sup>) distribution for 2015 over China. Data of NH<sub>3</sub> VCDs are  
579 derived from an improved version of the IASI dataset presented in Whitburn et al.<sup>40</sup> and  
580 Van Damme et al.<sup>53</sup>

581

582 **Figure 2 Comparison of NH<sub>3</sub> emissions with other published results and NH<sub>x</sub>**  
583 **deposition in mainland China during 2000-2015.** Studies addressing NH<sub>3</sub> emissions  
584 are colored with red symbols and NH<sub>x</sub> deposition colored with green symbols  
585 (references presented in this figure are listed in the SI TextS4). The red dotted line  
586 represents the NH<sub>3</sub> emission estimated in this study, and the green dotted line represents  
587 the NH<sub>x</sub> deposition synthesized by this study. The blue and grey shaded area indicates  
588 the 95% confidence interval of NH<sub>3</sub> emission evaluated by our study and NH<sub>x</sub>  
589 deposition on land calculated using data provided by Liu et al.<sup>17</sup> and Xu et al.<sup>6</sup>,  
590 respectively. Error bars of the symbols represent the uncertainties of their estimates,  
591 those symbols without error bars mean uncertainties unavailable or yet been discussed.

592

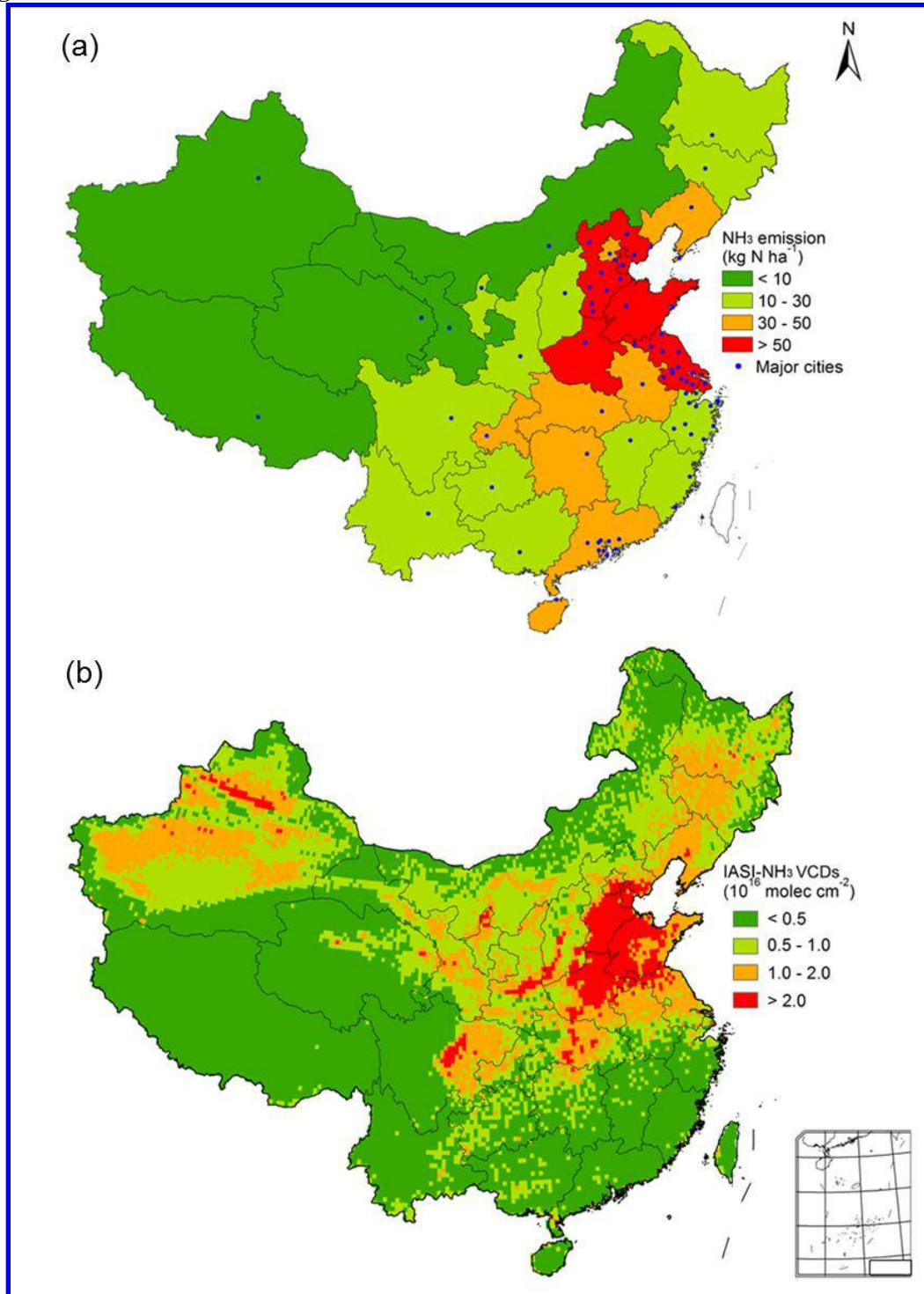
593 **Figure 3 Comparison with SO<sub>2</sub>&NO<sub>x</sub> emission on temporal trends.** The two solid  
594 lines show the molar ratios of (2SO<sub>2</sub>+NO<sub>x</sub>)/NH<sub>3</sub> and 2SO<sub>2</sub>/NH<sub>3</sub> in 2000-2015 in China.  
595 The dash line represents the molar ratio = 1. A ratio >1 represents NH<sub>3</sub> limitation to  
596 form the ammonium aerosol. While a ratio <1 represents NH<sub>3</sub> is available in abundance  
597 to form the ammonium aerosol contributing to Secondary Inorganic Aerosol formation  
598 (SIA), a substantial contributor to PM<sub>2.5</sub> concentrations. Data of SO<sub>2</sub>, NO<sub>x</sub> and NH<sub>3</sub>  
599 emission is based on MEPC,<sup>54</sup> Liu et al.<sup>37</sup> and our study, respectively.

600

601 **Figure 4 Validation by satellite observations (AIRS) on temporal trends.** The AIRS-  
602 NH<sub>3</sub> VCDs at 918 hPa from 2003 to 2015 are showed in pink dashed curves, with linear  
603 fits in solid lines. Data for AIRS-NH<sub>3</sub> VCDs was extracted from Warner et al.<sup>33</sup> and Van  
604 Damme et al.<sup>53</sup> The green dotted line represents the NH<sub>3</sub> emission estimated in this  
605 study.

606

607

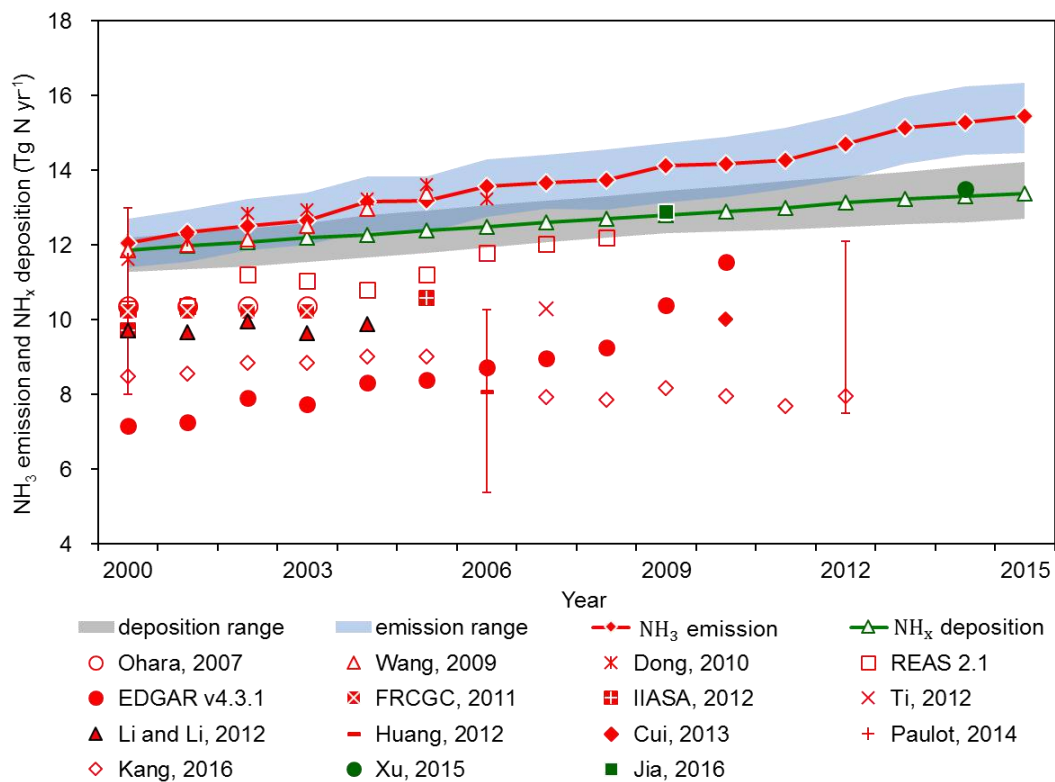
608 **Figure 1**

609

610

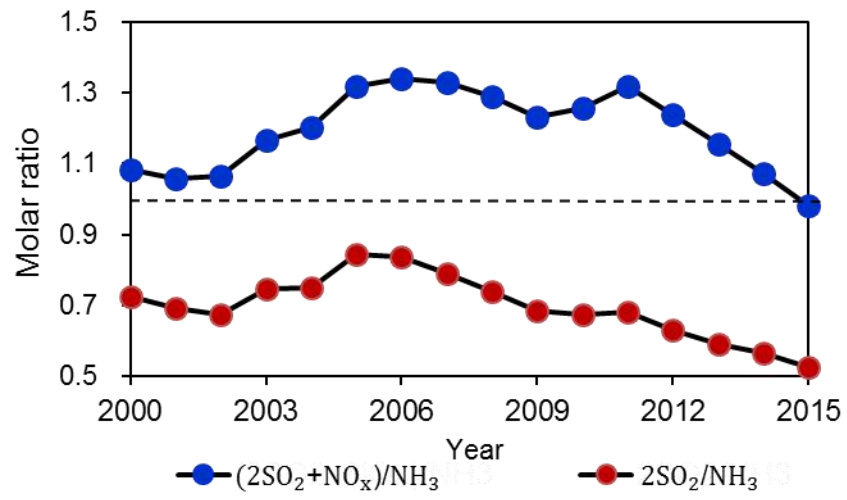
611

612 **Figure 2**



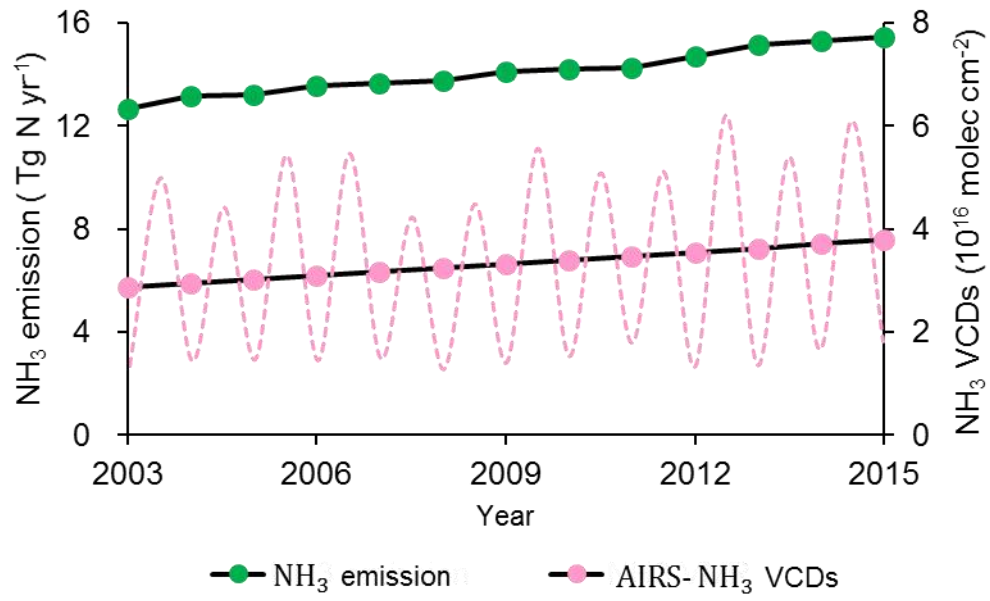
613

614

615 **Figure 3**

616

617

618 **Figure 4**

619

620

